Deferasirox (ExJade): A Fluorescent Pro-Chelator Active Against Antibiotic Resistant Bacteria

Adam C. Sedgwick,[b,‡] Kai-Cheng Yan,[a,‡] Daniel N. Mangel,[b] Ying Shang,[a] Axel Steinbrueck,[b] Hai-Hao Han,[a] James T. Brewster II,[b] Xi-Le Hu,[a] Dylan W. Snelson,[b] Vincent M. Lynch,[b] He Tian,[a] Xiao-Peng He,[a,*] and Jonathan L. Sessler[b,*]

[a]*Key Laboratory for Advanced Materials and Joint International Research Laboratory of Precision Chemistry and Molecular Engineering, Feringa Nobel Prize Scientist Joint Research Center, School of Chemistry and Molecular Engineering, East China University of Science and Technology, 130 Meilong Rd., Shanghai 200237, China;*

[b]*Department of Chemistry, The University of Texas at Austin, 105 East 24th Street-A5300, Austin, Texas 78712-1224, United States*

Abstract: Deferasirox, **ExJade**, an FDA-approved treatment for iron overload disorders has been shown to inhibit the growth of both gram-positive and -negative bacteria through iron (Fe(III)) chelation. Modification of the **ExJade** framework led to the identification of a new fluorescent platform **ExPh** and **ExBT**. Functionalization of the phenol moieties on **ExBT** with phosphate units afforded a ratiometric fluorescent pro-chelator (**ExPhos**), which was effective in the inhibition of two clinically relevant antibiotic-resistant bacteria, (MRSA (ATCC 43300) and VRE (ATCC 51299)), and allowed the fluorescent imaging of MRSA. Remarkably, this pro-chelation strategy proved selective towards bacteria with no cytotoxicity observed for **ExPhos** treated A549 cells (72 h incubation). This work represents a new pro-chelator antibiotic strategy that can be modified with a chosen reactive chemical trigger to provide a diagnostic signal in conjunction with a therapeutic response with a potential of minimal off-target toxicities.

Results and Discussion

Bacterial evolution, coupled with the global misuse of antibiotic treatments, has led to the emergence of antibiotic resistant bacteria (so-called “superbugs”) towards which numerous antibiotics are inactive.[1-3] This is spawning serious public health concerns, including fears of a potential return to the pre-antibiotic era.[4] Cost effective strategies for overcoming antibiotic resistance and new agents that operate via novel mechanisms of action may help alleviate some of these concerns. Recently, researchers have begun to exploit siderophore-mediated iron uptake pathways using natural or synthetic Fe(III) chelators in an attempt to interfere with bacterial Fe(III) acquisition and augment host “nutritional immunity” antibacterial mechanisms.[5-9] Here we report an iron chelation-based approach based on the Deferasirox (**ExJade**) skeleton that inhibits the growth of both gram-positive and -negative bacteria through Fe(III) chelation. The unique inherent fluorescent nature of the **ExJade** scaffold also

allows for the fluorescence-based optical imaging of Methicillin-resistant *Staphylococcus aureus* MRSA.

Recent efforts with the FDA-approved iron chelator **ExJade** have demonstrated its ability to act as a chemotherapeutic, insecticide, and antifungal agent; however, minimal efforts apparently have been devoted to exploring its potential as an antimicrobial agent.[10-14] We were thus keen to explore whether **ExJade** and its derivatives might provide a platform for the development of new antimicrobial agents. Specifically, we sought to test whether **ExJade** alone or after suitable functionalization would display attractive antimicrobial properties. With this goal in mind, **ExJade** and its derivatives were prepared (Fig. 1; cf. SI for synthesis).

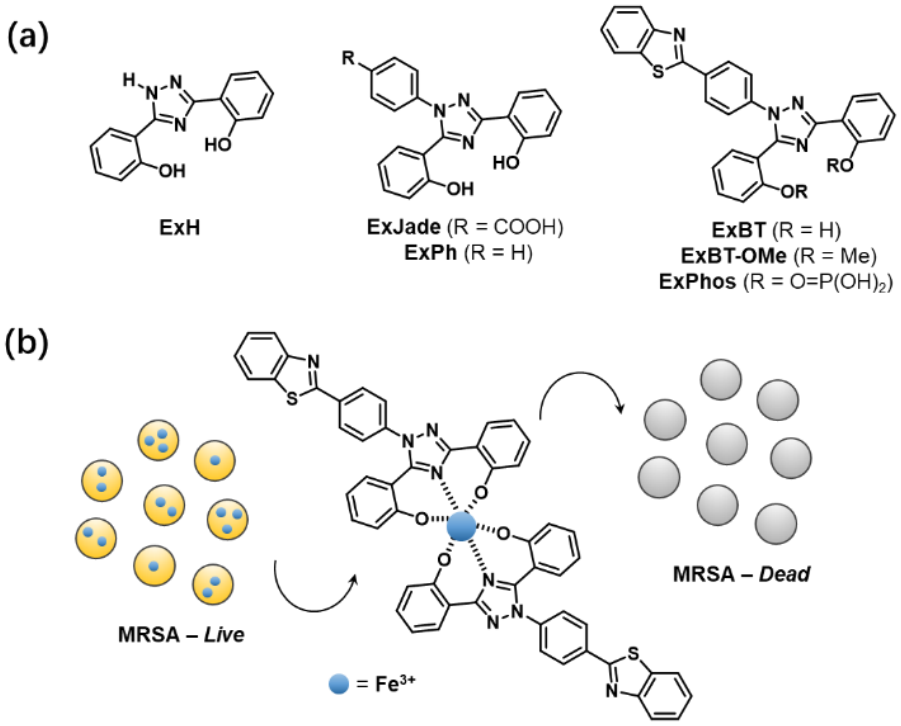

Figure 1 - (a) Structure of the **ExJade**-based derivatives developed in this study. (b) Schematic illustration of the antimicrobial effect of **ExBT** for Methicillin-resistant *Staphylococcus aureus* (MRSA), a clinically prevalent superbug, through the Fe(III)-chelating mechanism.

With the above goal in mind, several new **ExJade** derivatives, designed to control solubility and modulate the intrinsic electronic features, namely **ExPh**, **ExPh-OMe**, **ExH**, **ExBT**, **ExBT-OMe** and **ExPhos** (Fig. 1), were prepared (cf. ESI for synthesis). Unexpectedly, two of these derivatives, **ExPh** and **ExBT,** were found to display aggregation induced emission (AIE)-like properties in aqueous media (Figure 2).[15-16] Specifically, insoluble aggregates (as confirmed by DLS; cf. SI – Fig. S1) formed in water, leading to a strong fluorescence emission with a large Stokes shift (> 150 nm). Single crystal X-ray diffraction (XRD) analysis for **ExPh** and **ExBT** revealed strong intramolecular and intermolecular hydrogen bonding interactions, which is indicative of an excited state proton transfer based system (Figure 2a and 2b).[17,18-25] Further analysis of the crystal packing diagram revealed that both **ExPh** and **ExBT** exists in a slip-stacking orientation, which is known to augment rigidity in AIEgens since it serves to restrict intramolecular rotation (RIR) and enhance the fluorescence-based emission intensity (See ESI

– Fig. S2-5).[26-27] In marked contrast to what is seen in aqueous environments, solutions of **ExPh** and **ExBT** in most common organic solvents (See SI Fig. S6-9 – for solvents tested) display no appreciable emission.

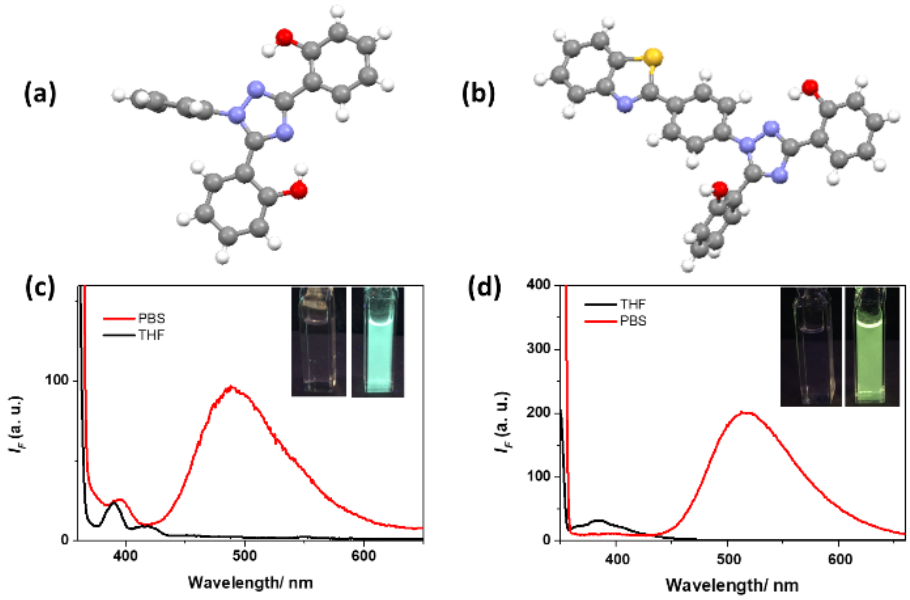

Figure 2 - (a) Ball and stick crystal structure of **ExPh**. (b) Ball and stick crystal structure of **ExBT**. (c) Fluorescence spectra of **ExPh** (10 μM) in **THF** and **PBS** (pH = 7.40); λ_{ex} = 300 nm. (d) Fluorescence spectra of **ExBT** (10 μM) in **THF** and **PBS** (pH = 7.40); λ_{ex} = 350 nm. CCDC 1967984 (**ExPh**); CCDC 1967981 (**ExBT**).

In an attempt to elucidate in greater detail the origins of the fluorescence displayed by **ExPh** and **ExBT** under conditions favoring aggregation, the derivatives, **ExPh-OMe**, **ExBT-OMe** and non-*N* phenyl functionalized **ExH**, were studied.[22,23] In both, aqueous and organic media, **ExH** was found to display strong fluorescence. This led us to believe the free rotation of the Ph unit effectively quenches the excited state fluorescence of **ExPh** and **ExBT**, a phenomenon known as the free rotor effect (see SI – Figs. S10-11).[26] Upon blocking each phenol unit present on **ExPh** and **ExBT** with a methyl group (to give **ExPh-OMe** and **ExBT-OMe**), a significant blue-shift in the emission maximum was seen (cf. SI- Fig. S12-15). Such changes in the emission features are consistent with the contention that the free form of the phenol is required for efficient ESIPT.[17]

No significant fluorescence quenching was seen upon changing the solvents in which **ExPh-OMe** and **ExBT-OMe** were analyzed – DMSO, PhMe, THF, DCM, acetone, MeCN, MeOH and PBS**.** On this basis we suggest that the ESIPT process is heavily affected by the free rotor effect.[28-29] In addition, significant solvatochromism was observed for both **ExPh-OMe** and **ExBT-OMe**, which leads us to suggest that a type of intramolecular charge transfer (ICT) process[30] is additionally involved in mediating the fluorescence features of these **ExJade** derivatives. This putative ICT phenomenon has been observed in structurally similar *N*-phenylpyrrole analogues.[31-32] Further support for the proposed aqueous induced aggregation mechanism invoked in the case of **ExPh** and **ExBT-OMe** came from studies of the parent system, **ExJade**. In the solid-state **ExJade** fluoresces;[33] however, it does not do so in aqueous solution, presumably as the result of its good solubility at neutral pH (See SI - Figure S16-17).

In the event, **ExPh** and **ExBT** proved to be highly emissive in aqueous media, making these species of interest in terms of the potential optical imaging of bacteria and other organisms.

Metal chelators, including **ExJade**, have begun to raise safety concerns owing to their off-target metal chelation, which can result in unwanted toxicities.[34-35] This has led to explorations of protected versions of chelators, often referred to as "pro-chelators".[36-40] These molecules are designed so in the presence of a disease-related stimulus, the metal binding site will be unmasked and that metal chelation will occur at the desired location. To the extent it is achieved, this high level of therapeutic precision serves to minimalize systemic toxicity. Nearly without exception, metal chelators and pro-chelators that have been studied in the context of biological applications are inherently non-fluorescent. As a result, the addition or conjugation of a fluorophore is necessary to visualize their cellular location. A related approach involves attaching a fluorophore to a pro-chelator that serves to report on the unmasking process.

We thus envisaged the inherent fluorescence of **ExJade** derivatives provides a unique multifunctional "molecular platform" that can be used to develop a fluorescence responsive pro-chelator active against antibiotic resistant bacteria. This system permits both detection and treatment with little synthetic investment. As a result, this strategy was explored using **ExBT**, which displayed optical characteristics deemed suitable for fluorescence imaging (λ_{ex} > 350 nm). Phosphate is an essential nutrient for bacterial growth and phosphatases are expressed in a range of bacteria.[41-43] **ExPhos** was thus developed to act as a phosphatase-responsive pro-chelator active against antibiotic resistant bacteria with minimal off-target toxicities. The pro-chelator function was not expected to manifest in the case of the control system, **ExBT-OMe**.

As expected and previously seen for **ExJade**,[44] the addition of increasing concentrations of Fe(III) (as the $FeCl_3$ salt) to both **ExBT** (15 μM) and **ExJade** (15 μM) led to a gradual increase in their respective UV-Vis absorption intensities, along with a color change from clear to purple (Fig. S18) Fluorescence experiments revealed a concentration-dependent quenching of the **ExBT** fluorescence (Fig. 3a), a common observation for Fe(III) chelation.[45] No change in the UV-Vis absorption or fluorescence was seen for either **ExBT-OMe** or **ExPhos** (Fig. 3b-c) (Fig. S18). This is consistent with the design expectation that a free phenol is need to chelate Fe(III) well.[44]

In the presence of alkaline phosphatase (ALP), a dose dependent change in fluorescence emission was observed (0 - 64 U), with a final fluorescence emission profile analogous to that of **ExBT** (Fig. 3d). This ratiometric change in fluorescence emission was ascribed to the gradual and stepwise dephosphorylation of **ExPhos**, which was confirmed by LC-MS analysis (See ESI – Figs. S19-S29). **ExPhos** solutions exposed to ALP (64 U ALP) were subsequently treated with increasing concentrations of Fe(III) (as the $FeCl_3$ salt). As expected for a system capable of chelating Fe(III), a quenching of the fluorescence intensity was observed (Fig. 3f). Based on these findings, we considered it likely that **ExPhos** could serve as an ALP-responsive Fe(III) pro-chelator.

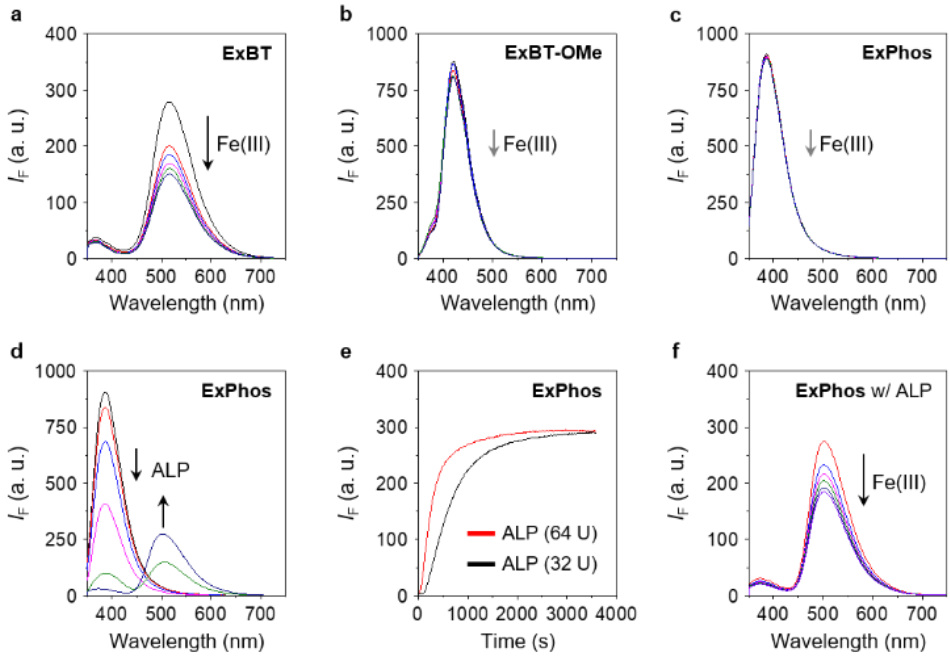

Figure 3 - Fluorescence spectra of (a) **ExBT** (15 µM), (b) **ExBT-OMe**, and (c) **ExPhos** (15 µM) recorded upon exposure to increasing Fe(III) concentrations (0-15 µM as the $FeCl_3$ salt). (d) Fluorescence changes of **ExPhos** (15 µM) with increasing alkaline phosphatase (ALP, 0-64 U). (e) Time-dependent change in the fluorescence-emission intensity at 505 nm observed when solutions containing **ExPhos** (15 µM) and ALP (two concentrations) were excited at 320 nm. (f) Fluorescence spectra of **ExPhos** (15 µM) preincubated with 64 U of ALP recorded as a function of increasing Fe(III) (0-15 µM). All measurements were carried out in deionized water.

With the photophysical properties identified, the bacterial inhibitory effect of the present **ExJade** derivatives were then evaluated. Initial tests were focused on two Gram-negative, ESKAPE bacteria,[46] *Pseudomonas aeruginosa* (ATCC 27853) and *Klebsiella pneumoniae* (ATCC 13883). Arbekacin, an FDA-approved aminoglycoside-based antibiotic, was used as positive control. **ExJade**, **ExPh**, **ExBT**, and **ExPhos** were found capable of inhibiting the growth of these two bacterial strains in a statistically significant manner (See ESI – Figs. S30-31).

More importantly, two clinically relevant gram-positive, drug-resistant bacteria, methicillin-resistant *Staphylococcus aureus* (MRSA, ATCC 43300) and vancomycin-resistant *Enterococcus faecalis* (VRE, ATCC 51299) with high ALP activity (Fig. S32) were then used to evaluate further the therapeutic potential of these **ExJade** derivatives. Again, arbekacin was used as a positive control. To our delight, strong inhibitory activities were observed for the suppression of these "superbugs" with a potency comparable to that of arbekacin (Fig. 4). The observed inhibition of VRE is of particular significance since there are few clinically available treatments for this multidrug-resistant bacterium.

The pre-incubation with increasing concentrations of Fe(III) led to a corresponding decrease in the inhibitory activity (Figs. S33, S34) including no appreciable inhibitory activity seen for either MRSA or *Pseudomonas aeruginosa* in the case of the control system **ExBT-OMe**. This observation confirms the Fe(III) chelation dependent inhibitory activity. Due to the Fe(III)

chelation dependent nature of the **ExJade** derivatives and to illustrate their potential "real life" utility, the inhibitory activity of **ExBT** and **ExPhos** against MRSA were evaluated in a blood containing medium consisting of agar and defibrillated amniotic blood.[47] Remarkably, no adverse effect was seen, with the inhibitory activity of **ExBT** and **ExPhos** remaining strong (Fig. S35). In addition, no significant cytotoxicity was observed for **ExPhos** towards A549 cells, providing an initial indication that the **ExJade**-based pro-chelation approach reported here may prove selective towards bacteria (See ESI – Fig. S36).

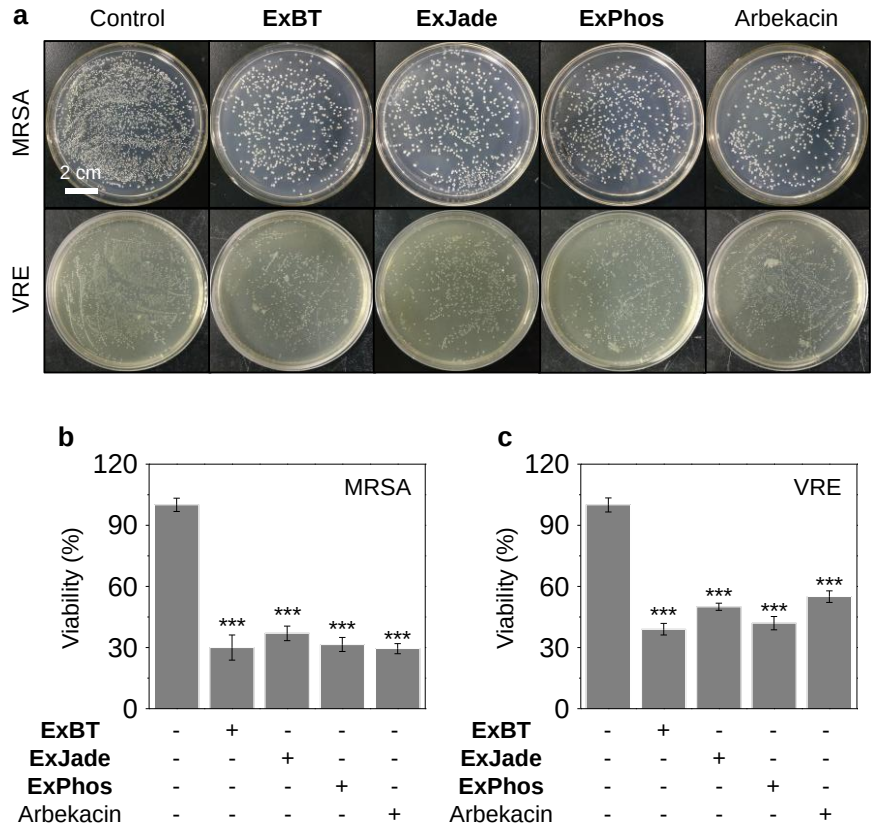

Figure 4 - (a) MRSA (ATCC 43300) colonies on Luria-Bertani (LB) tryptone agar plates and VRE (ATCC 51299) colonies on Brain-Heart Infusion (BHI) tryptone agar plates before and after treatment with **ExBT**, **ExJade**, **ExPhos**, and arbekacin (15 μM). Cell viability of (b) MRSA (ATCC 43300) and (c) VRE (ATCC 51299) before and after treatment with **ExBT**, **ExJade**, **ExPhos**, and arbekacin (15 μM).

Lastly, to determine whether the present **ExJade** derivatives might have a role to play as fluorescence imaging agents and theranostic agents, MRSA was incubated separately with **ExBT** and **ExPhos**; both compounds produced bright fluorescence in bacteria (Fig. 5a) Interestingly, the pre-treatment of MRSA with Phosphatase Inhibitor cocktail A (sodium fluoride, sodium pyrophosphate, β-glycerophosphate and sodium orthovanadate) led to an inhibitor concentration dependent decrease in the fluorescence emission intensity (Fig. 5a and Fig. 5b). This finding further confirms our contention that **ExPhos** is a pro-chelator that is activated under conditions of use *via* a phosphatase-mediated pathway.

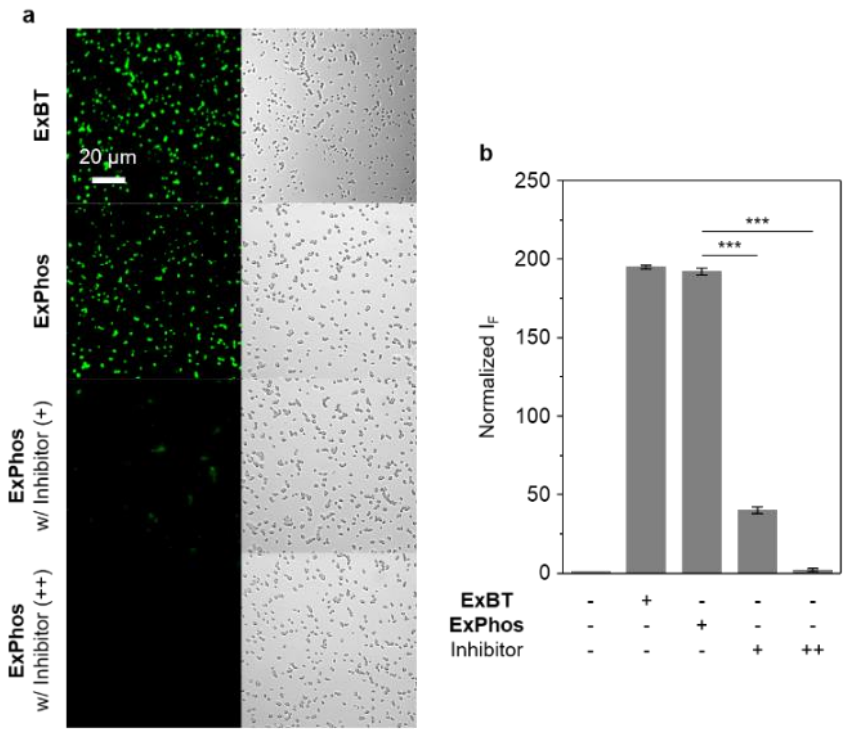

Figure 5 - (a) Confocal Laser-Scanning Microscope (CLSM) images (left: fluorescence images; right: bright-field images) of MRSA (ATCC 43300) treated with **ExBT** (40 µM), **ExPhos** (40 µM), or **ExPhos** pretreated with different concentrations of a phosphatase inhibitor cocktail A (+ 50 µM sodium fluoride, 10 µM sodium pyrophosphate, 10 µM β-glycerophosphate, and 10 µM sodium orthovanadate; ++: 100 µM sodium fluoride, 20 µM sodium pyrophosphate, 20 µM β-glycerophosphate and 20 µM sodium orthovanadate). (b) Normalized fluorescence intensities of the fluorescent imaged systems. ***P<0.001.

In summary, **ExJade**, an FDA-approved treatment for iron overload disorders has been identified to inhibit the growth of both gram-positive and -negative bacteria through iron (Fe(III)) chelation. The modification of **ExJade** revealed a new fluorescent framework that was shown effective in the inhibition of two clinically relevant antibiotic-resistant bacteria (MRSA (ATCC 43300) and VRE (ATCC 51299)), while also displaying an ability to image MRSA. This work highlights a pro-chelator strategy that exploits the unique inherent fluorescence nature of the **ExJade** scaffold while showing how this core can be modified with a chosen reactive chemical trigger to provide a diagnostic signal in conjunction with a therapeutic response.

Acknowledgements

The authors thank the National Natural Science Foundation of China (Nos. 21788102, 91853201, 21722801, 81673489 and 31871414), the Shanghai Municipal Science and Technology Major Project (No. 2018SHZDZX03), the International Cooperation Program of Shanghai Science and Technology Committee (No. 17520750100) and the Fundamental Research Funds for the Central Universities (222201717003) for financial support. The work in Austin was supported by the National Institutes of Health (R01 GM103790 to J.L.S.) and the Robert A. Welch Foundation (F-0018).

References

(1) Wright, P. M.; Seiple, I. B.; Myers, A. G., The Evolving Role of Chemical Synthesis in Antibacterial Drug Discovery. *Angew. Chem. Int. Ed.* **2014,** *53* (34), 8840-8869.

(2) von Bubnoff, A., Seeking new antibiotics in nature's backyard. *Cell.* **2006,** *127* (5), 867-869.

(3) Peeters, P.; Ryan, K.; Karve, S.; Potter, D.; Baelen, E.; Rojas-Farreras, S.; Rodriguez-Bano, J., The impact of initial antibiotic treatment failure: real-world insights in patients with complicated, health care-associated intra-abdominal infection. *Infect. Drug Resist.* **2019,** *12*, 329-343.

(4) Rugina, S., Resistance to Antimicrobians - A Global Problem with Sectoral Resolution. *J. Crit. Care Med.* **2018,** *4* (2), 47-49.

(5) Negash, K. H.; Norris, J. K. S.; Hodgkinson, J. T., Siderophore-Antibiotic Conjugate Design: New Drugs for Bad Bugs? *Molecules.* **2019,** *24* (18). DOI: 10.3390/molecules24183314

(6) Thompson, M. G.; Corey, B. W.; Si, Y. Z.; Craft, D. W.; Zurawski, D. V., Antibacterial Activities of Iron Chelators against Common Nosocomial Pathogens. *Antimicrob. Agents Chemother.* **2012,** *56* (10), 5419-5421.

(7) Miller, M. J.; Malouin, F., Microbial Iron Chelators as Drug Delivery Agents - The Rational Design and Synthesis of Siderophore-Drug Conjugates. *Acc. Chem. Res.* **1993,** *26* (5), 241-249.

(8) Mislin, G. L. A.; Schalk, I. J., Siderophore-dependent iron uptake systems as gates for antibiotic Trojan horse strategies against Pseudomonas aeruginosa. *Metallomics* **2014,** *6* (3), 408-420.

(9) Hennigar, S. R.; McClung, J. P., Nutritional Immunity: Starving Pathogens of Trace Minerals. *Am. J. Lifestyle Med.* **2016,** *10* (3), 170-173.

(10) Kielar, F.; Wang, Q.; Boyle, P. D.; Franz, K. J., A boronate prochelator built on a triazole framework for peroxide-triggered tridentate metal binding. *Inorg. Chim. Acta* **2012,** *393*, 294-303.

(11) Loza-Rosas, S. A.; Vazquez-Salgado, A. M.; Rivero, K. I.; Negron, L. J.; Delgado, Y.; Benjamin-Rivera, J. A.; Vazquez-Maldonado, A. L.; Parks, T. B.; Munet-Colon, C.; Tinoco, A. D., Expanding the Therapeutic Potential of the Iron Chelator Deferasirox in the Development of Aqueous Stable Ti(IV) Anticancer Complexes. *Inorg. Chem.* **2017,** *56* (14), 7788-7802.

(12) Puri, S.; Kumar, R.; Rojas, I. G.; Salvatori, O.; Edgerton, M., Iron Chelator Deferasirox Reduces Candida albicans Invasion of Oral Epithelial Cells and Infection Levels in Murine Oropharyngeal Candidiasis. *Antimicrob. Agents Chemother.* **2019,** *63* (4), DOI: 10.1128/AAC.02152-18

(13) Lui, G. Y. L.; Obeidy, P.; Ford, S. J.; Tselepis, C.; Sharp, D. M.; Jansson, P. J.; Kalinowski, D. S.; Kovacevic, Z.; Lovejoy, D. B.; Richardson, D. R., The Iron Chelator, Deferasirox, as a Novel Strategy for Cancer Treatment: Oral Activity Against Human Lung Tumor Xenografts and Molecular Mechanism of Action. *Mol. Pharmacol.* **2013,** *83* (1), 179-190.

(14) Gupta, P.; Jat, K.; Solanki, V. S.; Shrivastava, R., Synthesis and Antimicrobial Activity of some New N'-Arylidene-4-(3,5-Bis(2-Hydroxyphenyl)-1H-1,2,4-Triazole-1-yl) Benzohydrazides. *Indian J. Heterocycl. Chem.* **2017,** *27* (2), 151-156.

(15) Hong, Y. N.; Lam, J. W. Y.; Tang, B. Z., Aggregation-induced emission: phenomenon, mechanism and applications. *Chem. Commun.* **2009,** (29), 4332-4353.

(16) Qian, J.; Tang, B. Z., AIE Luminogens for Bioimaging and Theranostics: from Organelles to Animals. *Chem.* **2017,** *3* (1), 56-91.

(17) Sedgwick, A. C.; Wu, L. L.; Han, H. H.; Bull, S. D.; He, X. P.; James, T. D.; Sessler, J. L.; Tang, B. Z.; Tian, H.; Yoon, J., Excited-state intramolecular proton-transfer (ESIPT) based fluorescence sensors and imaging agents. *Chem. Soc. Rev.* **2018,** *47* (23), 8842-8880.

(18) Zhao, J. F.; Chen, J. S.; Liu, J. Y.; Hoffmann, M. R., Competitive excited-state single or double proton transfer mechanisms for bis-2,5-(2-benzoxazolyl)-hydroquinone and its derivatives. *Phys. Chem. Chem. Phys.* **2015,** *17* (18), 11990-11999.

(19) Hao, Y. C.; Chen, Y., Excited-state intramolecular single and double proton transfer emission of 2,5-bis(benzoxazol-2-yl)thiophene-3,4-diol. *Dyes Pigm.* **2016,** *129*, 186-190.

(20) Tang, K. C.; Chen, C. L.; Chuang, H. H.; Chen, J. L.; Chen, Y. J.; Lin, Y. C.; Shen, J. Y.; Hu, W. P.; Chou, P. T., A Genuine Intramolecular Proton Relay System Undergoing Excited-State Double Proton Transfer Reaction. *J. Phys. Chem. Lett.* **2011,** *2* (24), 3063-3068.

(21) Peng, C. Y.; Shen, J. Y.; Chen, Y. T.; Wu, P. J.; Hung, W. Y.; Hu, W. P.; Chou, P. T., Optically Triggered Stepwise Double-Proton Transfer in an Intramolecular Proton Relay: A Case Study of 1,8-Dihydroxy-2-naphthaldehyde. *J. Am. Chem. Soc.* **2015,** *137* (45), 14349-14357.

(22) Sahu, S.; Das, M.; Bharti, A. K.; Krishnamoorthy, G., Proton transfer triggered proton transfer: a self-assisted twin excited state intramolecular proton transfer. *Phys. Chem. Chem. Phys.* **2018,** *20* (42), 27131-27139.

(23) Das, M.; Sahu, S.; Krishnamoorthy, G., Tweaking the proton transfer triggered proton transfer of 3,5-bis(2-hydroxyphenyl)-1H-1,2,4-triazole. *Phys. Chem. Chem. Phys.* **2019,** *21* (28), 15669-15677.

(24) Sedgwick, A. C.; Dou, W. T.; Jiao, J. B.; Wu, L. L.; Williams, G. T.; Jenkins, A. T. A.; Bull, S. D.; Sessler, J. L.; He, X. P.; James, T. D., An ESIPT Probe for the Ratiometric Imaging of Peroxynitrite Facilitated by Binding to A beta-Aggregates. *J. Am. Chem. Soc.* **2018,** *140* (43), 14267-14271.

(25) Wu, L. L.; Han, H. H.; Liu, L. Y.; Gardiner, J. E.; Sedgwick, A. C.; Huang, C. S.; Bull, S. D.; He, X. P.; James, T. D., ESIPT-based fluorescence probe for the rapid detection of peroxynitrite 'AND' biological thiols. *Chem. Commun.* **2018,** *54* (80), 11336-11339.

(26) Lou, Z. R.; Hou, Y. Q.; Chen, K. P.; Zhao, J. Z.; Ji, S. M.; Zhong, F. F.; Dede, Y.; Dick, B., Different Quenching Effect of Intramolecular Rotation on the Singlet and Triplet Excited States of Bodipy. *J. Phys. Chem. C* **2018,** *122* (1), 185-193.

(27) Sivalingam, S.; Debsharma, K.; Dasgupta, A.; Sankararaman, S.; Prasad, E., Effect of Slip-Stack Self-Assembly on Aggregation-Induced Emission and Solid-State Luminescence in 1,3-Diarylpropynones. *Chempluschem* **2019,** *84* (4), 392-402.

(28) Vollmer, F.; Rettig, W., Fluorescence loss mechanism due to large-amplitude motions in derivatives of 2,2'-bipyridyl exhibiting excited-state intramolecular proton transfer and perspectives of luminescence solar concentrators. *Journal of Photochemistry and Photobiology a-Chemistry* **1996,** *95* (2), 143-155.

(29) Kim, S.; Seo, J.; Park, S. Y., Torsion-induced fluorescence quenching in excited-state intramolecular proton transfer (ESIPT) dyes. *J. Photochem. Photobio. A Chem.* **2007,** *191* (1), 19-24.

(30) Pannipara, M.; Asiri, A. M.; Alamry, K. A.; Arshad, M. N.; El-Daly, S. A., Synthesis, spectral behaviour and photophysics of donor-acceptor kind of chalcones: Excited state intramolecular charge transfer and fluorescence quenching studies. *Spectrochim. Acta A.* **2015,** *136*, 1893-1902.

(31) Yoshihara, T.; Druzhinin, S. I.; Demeter, A.; Kocher, N.; Stalke, D.; Zachariasse, K. A., Kinetics of intramolecular charge transfer with N-phenylpyrrole in alkyl cyanides. *J. Phys. Chem. A* **2005,** *109* (8), 1497-1509.

(32) Yoshihara, T.; Galievsky, V. A.; Druzhinin, S. I.; Saha, S.; Zachariasse, K. A., Singlet excited state dipole moments of dual fluorescent N-phenylpyrroles and 4-(dimethylamino)benzonitrile from solvatochromic and thermochromic spectral shifts. *Photochem. Photobiol. Sci.* **2003,** *2* (3), 342-353.

(33) Zhang, Y. J.; Yang, H. Y.; Ma, H. L.; Bian, G. F.; Zang, Q. G.; Sun, J. W.; Zhang, C.; An, Z. F.; Wong, W. Y., Excitation Wavelength Dependent Fluorescence of an ESIPT Triazole Derivative for Amine Sensing and Anti-Counterfeiting Applications. *Angew. Chem. Int. Ed.* **2019,** *58* (26), 8773-8778.

(34) Diaz-Garcia, J. D.; Gallegos-Villalobos, A.; Gonzalez-Espinoza, L.; Sanchez-Nino, M. D.; Villarrubia, J.; Ortiz, A., Deferasirox nephrotoxicity-the knowns and unknowns. *Nat. Rev. Nephrol.* **2014,** *10* (10), 574-586.

(35) Kontoghiorghes, G. J., Turning a blind eye to deferasirox's toxicity? *Lancet* **2013,** *381* (9873), 1183-1184.

(36) Hyman, L. M.; Franz, K. J., A cell-permeable fluorescent prochelator responds to hydrogen peroxide and metal ions by decreasing fluorescence. *Inorg. Chim. Acta* **2012,** *380*, 125-134.

(37) Zaengle-Barone, J. M.; Jackson, A. C.; Besse, D. M.; Becken, B.; Arshad, M.; Seed, P. C.; Franz, K. J., Copper Influences the Antibacterial Outcomes of a beta-Lactamase-Activated Prochelator against Drug-Resistant Bacteria. *ACS Infect. Dis.* **2018,** *4* (6), 1019-1029.

(38) Bakthavatsalam, S.; Sleeper, M. L.; Dharani, A.; George, D. J.; Zhang, T.; Franz, K. J., Leveraging -Glutamyl Transferase To Direct Cytotoxicity of Copper Dithiocarbamates against Prostate Cancer Cells. *Angew. Chem. Int. Ed.* **2018,** *57* (39), 12780-12784.

(39) Franks, A. T.; Franz, K. J., A prochelator with a modular masking group featuring hydrogen peroxide activation with concurrent fluorescent reporting. *Chem. Commun.* **2014,** *50* (77), 11317-11320.

(40) Wang, Q.; Franz, K. J., Stimulus-Responsive Prochelators for Manipulating Cellular Metals. *Acc. Chem. Res.* **2016,** *49* (11), 2468-2477.

(41) Sajid, A.; Arora, G.; Singhal, A.; Kalia, V. C.; Singh, Y., Protein Phosphates of Pahtogenic Bacteria: Role in Physiology and Virulence. *Annu. Rev. Microbiology,* **2015**, 69, 527-547.

(42) Braibant, M.; Content, J., The cell surface associated phosphatase activity of Mycobacterium bovis BCG is not regulated by environmental inorganic phosphate. *FEMS Microbiol. Lett.* **2001,** *195* (2), 121-126.

(43) Kriakov, J.; Lee, S. H.; Jacobs, W. R., Identification of a regulated alkaline phosphatase, a cell surface-associated lipoprotein, in Mycobacterium smegmatis. *J. Bacteriol.* **2003,** *185* (16), 4983-4991.

(44) Steinhauser, S.; Heinz, U.; Bartholoma, M.; Weyhermuller, T.; Nick, H.; Hegetschweiler, K., Complex formation of ICL670 and related ligands with Fe-III and Fe-II. *Eur. J. Inorg. Chem.* **2004,** (21), 4177-4192.

(45) Qu, X. Y.; Liu, Q.; Ji, X. N.; Chen, H. C.; Zhou, Z. K.; Shen, Z., Enhancing the Stokes' shift of BODIPY dyes via through-bond energy transfer and its application for Fe3+-detection in live cell imaging. *Chemical Communications* **2012,** *48* (38), 4600-4602.

(46) Mulani, M. S.; Kamble, E. E.; Kumkar, S. N.; Tawre, M. S.; Pardesi, K. R., Emerging Strategies to Combat ESKAPE Pathogens in the Era of Antimicrobial Resistance: A Review. *Front. Microbiol.* **2019,** *10*. DOI: 10.3389/fmicb.2019.00539

(47) Filipowicz, N.; Kaminski, M.; Kurlenda, J.; Asztemborska, M.; Ochocka, J. R., Antibacterial and antifungal activity of juniper berry oil and its selected components. *Phytother. Res.* **2003,** *17* (3), 227-231.